A&A 474, 1051–1059 (2007)
DOI: 10.1051/0004-6361:20078238

Astronomy & Astrophysics

Dielectronic recombination data for dynamic finite-density plasmas

XIII. The magnesium isoelectronic sequence

Z. Altun[1], A. Yumak[1], I. Yavuz[1], N. R. Badnell[2], S. D. Loch[3], and M. S. Pindzola[3]

[1] Department of Physics, Marmara University, Istanbul 34722, Turkey
e-mail: zikalt@superonline.com
[2] Department of Physics, University of Strathclyde, Glasgow G4 0NG, UK
[3] Department of Physics, Auburn University, Auburn, AL 36849, USA

Received 6 July 2007 / Accepted 5 September 2007

ABSTRACT

We have calculated total and partial final-state level-resolved dielectronic recombination (DR) rate coefficients for the ground and metastable initial levels of 21 Mg-like ions between Al^{+} and Xe^{42+}. This is the final part of the assembly of a level-resolved DR database necessary for modelling dynamic finite-density plasmas within the generalized collisional-radiative framework. Calculations have been performed in both *LS*- and intermediate coupling, allowing for $\Delta n = 0$ and $\Delta n = 1$ core-excitations from ground and metastable levels. Complementary partial and total radiative recombination RR coefficients have been calculated for the same ions viz. Al^{+} through Zn^{18+}, as well as Kr^{24+}, Mo^{30+}, and Xe^{42+}. Fitting coefficients which describe the total RR and DR rate coefficients (separately) are also presented here. Results for a selection of ions from this sequence are discussed, and compared with existing theoretical and experimental results. A full set of results can be accessed from the Atomic Data and Analysis Structure (ADAS) database or from the Oak Ridge Controlled Fusion Atomic Data Center (http://www-cfadc.phy.ornl.gov/data_and_codes). The complexity of further M-shell sequences, both from the atomic and modelling perspectives, renders this juncture a natural conclusion for the assemblage of the partial database. Further M-shell work, has and will, focus more on total rate coefficients, rather than partials, at least in the medium term.

Key words. atomic data – atomic processes – plasmas

1. Introduction

Dielectronic recombination (DR) is the process of resonant electron capture by an ion followed by radiative stabilization (Burgess 1964). DR is the dominant electron-ion recombination process in both photoionized and collisional plasmas (Ferland et al. 1998; Mazzotta et al. 1998).

DR is a major energy-loss mechanism in optically thin plasmas. Thus, accurate DR rate coefficients are important for interpreting and modelling the level populations and the ionization balance of these plasmas over a wide range of electron temperatures and densities, and plasma timescales. Accurate DR rate coefficients are essential for the reliable spectral diagnosis of non-equilibrium laboratory and astrophysical plasmas.

DR data are abundant for K-shell and L-shell ions. Most of the available and recommended DR rate coefficients for K-shell and L-shell ions, prior to a new programme initiated by Badnell et al. (2003), resulted from the primary and/or secondary work of Aldrovandi & Péquignot (1973), Shull & van Steenberg (1982), Nussbaumer & Storey (1983, 1984, 1987), Arnaud & Rothenflug (1985), Landini & Monsignori Fossi (1990, 1991), Arnaud & Raymond (1992), Jacobs et al. (1977a,b, 1979, 1980), Hahn (1989), and Mazzotta et al. (1998).

These previous results are usually for totals from the initial ground state only, often using single-configuration *LS*-coupling approximations or semi-empirical formulae or isoelectronic interpolations. To go beyond this picture and produce more accurate and reliable DR data, a new programme was started by Badnell et al. (2003) which focused on including DR contributions from both ground and metastable initial states, and taking into account the fine-structure transitions, like $2p_{3/2} \rightarrow 2p_{1/2}$, which are particularly important at photoionized plasma temperatures. Following the initiation of this programme, studies have been carried-out for the hydrogen through sodium-like isoelectronic sequences. The references for the papers covering these works are: hydrogen-like (Badnell 2006a), helium-like (Bautista & Badnell 2007), lithium-like (Colgan et al. 2004), beryllium-like (Colgan et al. 2003), boron-like (Altun et al. 2004), carbon-like (Zatsarinny et al. 2004a), nitrogen-like (Mitnik et al. 2004), oxygen-like (Zatsarinny et al. 2003), fluorine-like (Zatsariny et al. 2006), neon-like (Zatsarinny et al. 2004b), and sodium-like (Altun et al. 2006). Complementary radiative recombination rate coefficients have been calculated by Badnell (2006b). These (total) data have been used by Bryans et al. (2006) to determine new coronal ionization balances for all elements up to Zn, and they compare them in detail with those determined by Mazzotta et al. (1998).

Sophisticated calculations of DR rate coefficients have also been carried-out by Chen et al. (e.g. 1985, 1987, 2002) and by Gu (2003a,b, 2004). The wealth of information concerning DR rate coefficients for K-shell and L-shell ions is largely due to the co-operative and productive interplay between theory and experiment over the last decade. Electron beam ion trap (EBIT) and ion storage ring measurements have played a critical role in the development of modern theoretical methods for DR calculations. Review articles by Müller (1999) and by Savin & Laming (2002) make this point very clear.

While DR data are abundant for K-shell and L-shell ions, the situation for M-shell ions is very different. There are only a few studies concerning DR for M-shell ions in the literature. But, M-shell DR is expected to be important. Chandra and XMM Newton X-ray observations of active galactic nuclei have identified the part of the absorption spectrum in the 15−17 Å range as mainly being due to 2p → 3d inner shell transitions of iron ions with open M-shells. Such inner shell transitions have been observed in many other observations, as discussed by Lukić et al. (2007) and references therein.

Recently, Netzer et al. (2003), Netzer (2004) and Kraemer et al. (2004) examined the effects of low-temperature, or $\Delta n = 0$ core excitation, DR on the ionization balance of Fe M-shell ions in photoionized plasmas and they demonstrated the critical need for reliable DR rate coefficients for Fe M-shell ions. This is necessary in order to describe the transition array of inner-shell 2−3 lines seen in high resolution X-ray spectra of Seyfert Galaxies observed with XMM-Newton and Chandra. Netzer (2004) has concluded that without reliable Fe M-shell DR data, it is not possible to model photoionized plasmas where there are strong overlaps from 2−3 inner-shell transition lines of FeI – FeXVI superimposed on the spectra corresponding to H-like, He-like lines and inner-shell lines of silicon, sulphur and iron. A strong interest in M-shell DR rate coefficients and associated resonance spectrum has recently been emphasized by Lukić et al. (2007).

Several pioneering calculations on Mg-like ions in the literature are based on the formulation by Burgess (1964), with some modifications. Jacobs et al. (1977a) calculated DR rate coefficients for Fe^{14+} as part of their survey of Fe ions ranging from Fe^{8+} to Fe^{24+}. Similar later work addressed Si^{2+}, S^{4+} and Ca^{8+} & Ni^{16+}, Jacobs et al. (1977b, 1979, 1980), as part of their isonuclear studies on these elements. The main limitation of their approach (which was advanced at the time) was that only dipole autoionizing transitions were considered, along with only inner-electron radiative transitions.

Since then, Dube et al. (1985) have calculated dielectronic recombination rate coefficients for the ions Si^{2+}, Ar^{6+}, Fe^{14+} and Mo^{30+} within a single configuration *LS*-coupling scheme, including both $\Delta n = 0$ and $\Delta n = 1$ excitations from the 3s level. Subsequently, Dube & LaGattuta (1987) included $\Delta n = 1$ excitations from the 2p sub-shell. They also did some test calculations for excitations from the 1s and 2s sub-shells which led them to conclude that these contributions could be neglected. An early study which went beyond the Burgess model (1964) on a Mg-like ion was done by Badnell (1991) as part of his studies of DR rate coefficients for S^{q+} ($q = 1-5$) ions using the AUTOSTRUCTURE code (Badnell 1986, 1997).

These data form the basis of the Mg-like DR rate coefficients recommended by Mazzotta et al. (1998) viz. Si, Ar & Fe (Dube et al. 1985; Dube & LaGattuta 1987; and extended to lower temperatures following Mattioli 1988); S (Badnell 1991); Ca & Ni (Jacobs et al. 1980). Results for the other Mg-like ions (Al to Co) are based on the interpolation of these results (extrapolation in the case of Al), following Landini & Monsignori Fossi (1990, 1991).

Very recent multi-configuration Breit-Pauli (MCBP) AUTOSTRUCTURE calculations of the DR for the iron M-shell ions Fe^{13+} and Fe^{8+} – Fe^{12+} by Badnell (2006c,d) demonstrated the importance of DR for the accurate modelling of photoionized plasmas, especially in connection with the unresolved-transition-array problem (Netzer 2004). Recent experimental measurements by Schmidt et al. (2006) on Fe^{13+} at the Heidelberg heavy-ion test storage are also very timely in encouraging studies of electron-ion recombination studies for M-shell ions.

In this paper, we report on a comprehensive study of DR rate coefficients for Mg-like ions ranging from Al^{+} through Zn^{18+}, as well as Kr^{24+}, Mo^{30+}, and Xe^{42+}. We employ the MCBP method and impose the independent processes and isolated resonance approximations. Our calculations include core excitations from the ground and metastable states; this is essential to the description of a plasma for which the timescale of change in electron temperature and electron densities of the plasma is comparable with the lifetime of the metastable populations of its constituent ions. These populations may no longer be assumed to be in quasi-static equilibrium with the ground state. For these situations accurate population modelling DR from metastable states must be considered on an equal footing with the ground states. We report and archive final-state level-resolved DR rate coefficients. These are important for the collisional-radiative modelling of finite-density plasmas where stepwise ionization can significantly reduce the effective recombination rate coefficient, compared with its low-density limit (Burgess & Summers 1969).

The computational method for DR, described in detail by Badnell et al. (2003), has been used extensively to produce a database to meet the increasing demand from modern plasma diagnostics studies. Our calculations embrace a wide range of electron temperatures, $Z^2(10-10^7)$ K where Z is the electron target ion charge, for 21 Mg-like ions from Al to Xe. In calculating "M-shell" DR for these ions we have considered both $\Delta n = 0$ and $\Delta n = 1$ core excitations involving 2p, 3s and 3p subshells during the capture of the colliding electron. DR associated with $\Delta n = 0$ core excitations occurs at much lower temperatures and is the dominant recombination process in photoionized plasmas. However, we should note the importance of $2 \rightarrow 3$ $\Delta n = 1$ core excitations at high temperatures for high-Z ions.

Results are presented in both *LS*- and intermediate coupling approximations. We compute and compare *LS*-coupling results because as we progress into the M-shell it becomes increasingly demanding to carry out Breit-Pauli calculations. *LS*-coupling calculations are an order of magnitude less demanding than Breit–Pauli and so they enable us to investigate the role of various configurations and, ultimately, may be all that it is tractable. *LS*-coupling results are automatically generated in the course of the MCBP calculations.

We make comparisons of our intermediate coupling MCBP results with those currently recommended by Mazzotta et al. (1998) for plasma modelling. We also make comparison with the recent detailed storage ring measurements of Lukić et al. (2007) for Fe^{14+}.

The remainder of the paper is structured as follows: in Sect. 2 we give a brief description of the theory used, in Sect. 3 we compare our velocity-averaged DR cross sections with the measurements made at storage rings utilizing electron-coolers, and in Sect. 4 we present DR and RR rate coefficients for the magnesium isoelectronic sequence and compare them with the existing results for a selection ions. We conclude with a brief summary.

2. Theory

The theoretical details of our DR calculations have already been described (Badnell et al. 2003). Here we outline only the main points. The AUTOSTRUCTURE code (Badnell 1986, 1997) was used to calculate energy levels, radiative and autoionization rates in the *LS*- and intermediate coupling (MCBP) approximations using non-relativistic (up to Zn) and semi-relativistic (from Zn)

radial functions. There are options to use either Slater-Type-Orbital (STO) or Thomas-Fermi-Dirac-Amaldi (TFDA) type model for the calculations of radial orbitals. We have chosen TFDA type model potential for DR calculations of Mg-like ions.

The autoionization rates are calculated in the isolated resonance approximation using a distorted-wave approximation where both electron-electron and electron-photon interactions are treated to first order. This enables the generation of final-state level-resolved and total dielectronic recombination rate coefficients in the independent processes approximation, where the interference between the radiative recombination and the dielectronic recombination processes are ignored. Although this has been found to be only a very small effect for the total rate (Pindzola et al. 1992), more recent studies of partial recombination cross sections for Li-like fluorine F^{6+} (Mitnik et al. 1999) predict some interference between these processes for weak partial cross sections.

The dielectronic capture processes for (outer-shell) $n = 3$ electrons of the ground state of Mg-like ions can be described by the following reactions (where we have suppressed the $1s^2$ label)

$$2s^2 2p^6 3s^2\,{}^1S_0 + e^- \rightarrow 2s^2 2p^6 3l' 3l'' nl, \quad (1)$$

for $\Delta n = 0$ core-excitations and, for $\Delta n = 1$, by

$$2s^2 2p^6 3s^2\,{}^1S_0 + e^- \rightarrow 2s^2 2p^6 3l' 4l'' nl, \quad (2)$$

and similarly for the $3s3p\,{}^3P_J$ metastable levels. All $n = 3$ promotions were treated at the same time, i.e. the full 3:3: and 3:4: N-electron target and core complexes were included. For these transitions, l and n values were included up to 15 and 25, respectively. For higher values of n, up to 1000, the bound Rydberg orbital is approximated by a zero-energy continuum orbital utilizing quantum-defect theory (Badnell et al. 2003).

The dielectronic capture processes for (inner-shell) 2p core-excitations can be written as (for the ground level)

$$2s^2 2p^6 3s^2\,{}^1S_0 + e^- \rightarrow 2s^2 2p^5 3l' 3l'' 3l''' nl, \quad (3)$$

and similarly for the metastables. The target/core was again described by all configurations belonging to the 3:3: complex, except $3d^2$ now, together with the 2p-hole configurations with $l' + l'' + l''' \leq 3$. The values of l and n were taken up to 7 and 25, respectively, and the small contribution from higher values of n via the quantum-defect theory approximation. Test calculations show that the contribution to the total DR rate coefficient from 2s promotions is ~1%, and so we do not consider them further.

The dielectronic recombination rate coefficient from an initial metastable state ν to a final-state i is given by

$$\alpha_{i\nu} = \left(\frac{4\pi a_0^2 I_H}{k_B T_e}\right)^{3/2} \sum_j \frac{\omega_j}{2\omega_\nu} e^{-E_c/k_B T_e} \times \frac{\sum_l A^a_{j\rightarrow\nu,E_c l} A^r_{j\rightarrow i}}{\sum_h A^r_{j\rightarrow h} + \sum_{m,l} A^a_{j\rightarrow m,E_c l}}, \quad (4)$$

where ω_j is the statistical weight of the $(N+1)$-electron doubly-excited resonance state j, ω_ν is the statistical weight of the N electron target state and the autoionization (A^a) and radiative (A^r) rates are in inverse seconds. Here, E_c is the energy of the continuum electron of angular momentum l, which is fixed by the position of the resonances, and I_H is the ionization potential energy of the hydrogen atom, k_B is the Boltzmann constant, T_e is the electron temperature and $(4\pi a_0^2)^{3/2} = 6.6011 \times 10^{-24}$ cm^3. Note, in determining total DR rate coefficients, we sum over only final states which are stable against autoionization. Calculations were carried-out using the AUTOSTRUCTURE computer code which is implemented within the ADAS suite of programs as ADAS701.

For $\Delta n = 0$ core-excitations, the resonance energies are empirically adjusted so that the series limits match the $3 \rightarrow 3$ core-excitation energies obtained from the NIST Atomic Spectra Database (v. 3). Accurate resonance energies are particularly important for the calculations of low-temperature dielectronic recombination rate coefficients. Separate calculations were performed for the outer-shell ($n = 3$) and inner-shell (2p) promotions. Finally, *LS* - and intermediate-coupling dielectronic recombination rate coefficients for different core-excitations were archived according to the *adf09* format, to be added to the existing ADAS database (Summers 2003).

The theoretical details of our RR calculations have already been described by Badnell (2006b), who considered all initial sequences up-to and including Na-like, and for the same elemental range here. Briefly, we describe the Mg-like target by the 6 configurations of the $n = 3$ complex and consider capture to all nl up to $n = 1000$ and $l = 200$, with $l \geq 4$ treated hydrogenically. Partial RR rate coefficients are tabulated according to the ADAS *adf48* format.

3. Results

In Fig. 1 we compare our MCBP intermediate coupling velocity-averaged dielectronic recombination cross sections for Fe^{14+}, forming Fe^{13+} via $3 \rightarrow 3$ ($\Delta n = 0$) core-excitations, with measurements carried-out using the heavy-ion Test Storage Ring at the Max-Planck-Institute for Nuclear Physics in Heidelberg, Germany by Lukić et al. (2007). We have convoluted our DR cross sections (× velocity) with the energy spread corresponding to temperatures $k_B T_\perp = 6.20$ meV and $k_B T_\parallel = 0.048$ meV. To account for field ionization effects we eliminated all resonances with $n \geq 80$, which is the experimental cutoff estimated by Lukić et al. (2007). Although there is some uncertainties in the resonance strengths in the experimental measurements due to the difficulties associated with the determination of the non-resonant background, the overall agrement between theory and experiment is quite good. There may be additional uncertainty in the experimental results from a possible contamination of Fe^{14+} beam by metastable $^3P_0$ ions.

Resonances below the $3s^2\,{}^1S_0 \rightarrow 3s3p(^1P_J)nl$ series limit, at approximately 43.4 eV, are predominantly due to capture to $3s3p(^{1,3}P_J)nl_j$, $3p^2(^1S_0, ^1D_2, ^3P_J)nl_j$ and $3s3d(^1D_2, ^3D_J)nl_j$. The low-lying resonances near threshold correspond to the doubly-excited states $3s3p(^{1,3}P)10l$, $3d^2(^3F_J)4f$ and 4g, $3p3d(^3P_J)5p$, and $3p3d(^3D_3)5p$. The main puzzle is the discrepancy observed just below the series limit itself. There is no identifiable physical mechanism to source it – results are insensitive to the expected field ionization. Similar behaviour was noted for Fe^{13+} by Badnell (2006c). However, no such discrepancy was noted for Fe^{15+} (Altun et al. 2006) and, most recently, none is noted for $Fe^{7+,8+}$ (Badnell 2006d & unpublished; and Schmidt 2007).

Detailed results of our calculations, done in both *LS* - and intermediate-coupling and for both $\Delta n = 0$ and $\Delta n = 1$ core excitations, are available on the web (`http://www-cfadc.phy.ornl.gov/data_and_codes`) in the ADAS *adf09* format (Summers 2003). They provide final-state resolved dielectronic recombination rate coefficients from both the ground and metastable initial states into final *LS* terms

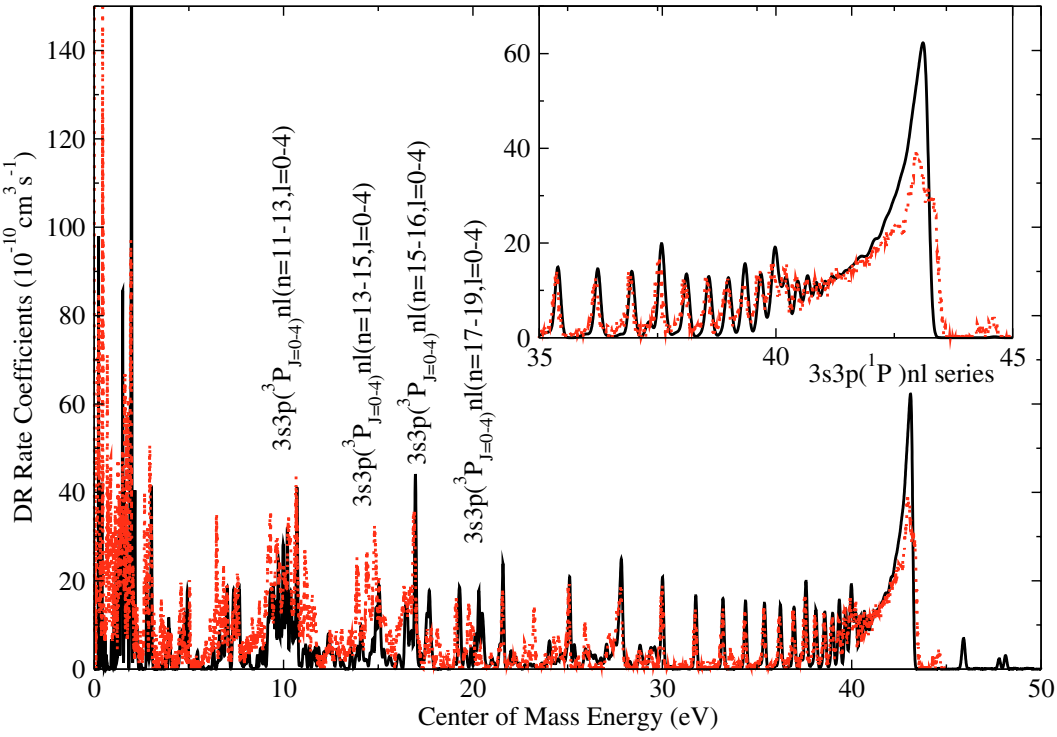

Fig. 1. Present intermediate coupling velocity-averaged MCBP dielectronic recombination cross sections for Fe^{14+}, as a function of center-of-mass collision energy in the range 0 to 45 eV. The resonances in this range are mostly associated with $n = 3 \rightarrow 3$ ($\Delta n = 0$) core-excitations corresponding to the doubly excited states $3s3p(^1P)nl$ with $n \geq 8$. The solid line denotes our intermediate coupling MCBP results and the dotted line denotes the experimental results of Lukić et al. (2007). Our DR cross sections (×velocity) have been convoluted with the experimental energy spread of Lukić et al. (2007), corresponding to temperatures $k_B T_\perp = 6.20$ meV and $k_B T_\parallel = 0.048$ meV.

or *LSJ* levels in a manner useful to fusion and astrophysical modellers.

The total ($\Delta n = 0$ plus $\Delta n = 1$) DR rate coefficients were fitted using the formula

$$\alpha_{\rm DR} = \frac{1}{T^{3/2}} \sum_{i=1}^{n} c_i e^{-E_i/T}, \quad (5)$$

where n ranges from 3 to 6, depending on the ion. Here, T and E_i are in units of temperature (K) and the rate coefficient $\alpha_{\rm DR}$ is in units of cm^{3}s^{-1}. Our fits are accurate to better than ≈5% for all ions in the temperature range $Z^2(10–10^7)$ K, where Z is the residual charge of the initial ion. In fact, this 5% applies only over limited energy ranges where the DR has a local minimum. The accuracy is typically better than 1% over the broad range of temperatures where DR dominates in both collision dominated and photoionized plasmas. In Table 1, we present the DR fit coefficients for each member of the magnesium isoelectronic sequence considered.

The total RR rate coefficients were fitted using the formula

$$\alpha_{\rm RR}(T) = A \times \left[\sqrt{T/T_0} \left(1 + \sqrt{T/T_0}\right)^{1-B} \left(1 + \sqrt{T/T_1}\right)^{1+B} \right]^{-1}, \quad (6)$$

where, for low-charge ions, B is replaced as

$$B \rightarrow B + C \exp(-T_2/T). \quad (7)$$

Here, $T_{0,1,2}$ are in units of temperature (K) and the rate coefficient $\alpha_{\rm RR}(T)$ is in units of cm^3 s^{-1}. (The units of A are also cm^3 s^{-1}, while B and C are dimensionless.) The fits are accurate to better than 1% over $Z^2(10^1–10^7)$ K for multiply charged ions, 5% for singly and doubly ionized, and have the correct asymptotic forms outside of this temperature range. In Table 2, we present the RR fit coefficients for each member of the magnesium isoelectronic sequence considered.

As an example of the final-state level-resolved (RR+DR) rate coefficients that have been obtained from the MCBP calculations, we present in Table 3 results from the initial $2s^22p^63s^2(^1S_0)$ ground state of Fe^{14+} to the lowest 24 levels of Fe^{13+}. The rest of the results readily accessible from the web (`http://www-cfadc.phy.ornl.gov/data_and_codes`).

Total dielectronic recombination rate coefficients for all ions considered in this paper are obtained by summing the contributions from the $3 \rightarrow 3$ ($\Delta n = 0$), $2 \rightarrow 3$, and $3 \rightarrow 4$ ($\Delta n = 1$) core-excitations.

In Fig. 2 we compare our total MCBP dielectronic recombination rate coefficients for Fe^{14+}, as a function of electron temperature, with previous results from the literature. The fit data provided by Mazzotta et al. (1998) is apparently based on the high temperature ($\gtrsim 3 \times 10^6$ K) results of Dube et al. (1985), for 3s promotions, and Dube & LaGattuta (1987), for 2p promotions, and extended to lower temperatures following Mattioli (1988). The Mazzotta et al. (1998) results are in close agreement with those presented by Arnaud & Raymond (1992), which are based on the results of Jacobs et al. (1977a) and which did not allow for 2p promotions. Like Mazzotta et al. (1998), Arnaud & Raymond (1992) indicate that they also allowed for 2p promotions, following Dube & LaGattuta (1987). However, all four sets of results: Mazzotta et al. (1998), Arnaud & Raymond (1992), Jacobs et al. (1977a) and Dube et al. (1985) are in close agreement with each other (and so we only show one curve in the figure) *and* with our contribution from 3s promotions *alone*. *But*,

Table 1. Fitting coefficients (see Eq. (5)) c_i (cm^3 s^{-1} K$^{3/2}$) and E_i(K) for ground state total DR rate coefficients of Mg-like ions. $X(Y)$ means $X \times 10^Y$.

Ion	c_1	c_2	c_3	c_4	c_5	c_6
Al^{1+}	4.495(−7)	2.610(−6)	3.816(−3)	5.803(−4)	···	···
Si^{2+}	2.930(−6)	2.803(−6)	9.023(−5)	6.909(−3)	2.582(−5)	···
P^{3+}	6.763(−6)	3.864(−6)	3.456(−5)	2.562(−4)	1.430(−2)	2.623(−4)
S^{4+}	9.571(−6)	6.268(−5)	3.807(−4)	1.874(−2)	5.526(−3)	···
Cl^{5+}	1.298(−5)	6.784(−5)	2.295(−4)	3.446(−3)	3.153(−2)	2.824(−3)
Ar^{6+}	5.219(−5)	3.268(−4)	1.514(−3)	5.551(−3)	4.596(−2)	7.266(−3)
K^{7+}	9.176(−5)	1.519(−4)	2.585(−3)	1.364(−2)	5.097(−2)	1.478(−2)
Ca^{8+}	1.697(−4)	7.725(−4)	5.140(−3)	3.397(−2)	4.806(−2)	2.745(−2)
Sc^{9+}	1.474(−4)	2.209(−3)	7.660(−3)	8.018(−2)	1.978(−2)	4.575(−2)
Ti^{10+}	8.273(−4)	2.017(−3)	1.378(−2)	1.013(−1)	1.471(−2)	7.139(−2)
V^{11+}	2.311(−4)	2.759(−3)	1.129(−2)	5.990(−2)	8.430(−2)	1.084(−1)
Cr^{12+}	5.905(−5)	9.600(−4)	6.084(−3)	1.501(−1)	3.658(−2)	1.516(−1)
Mn^{13+}	2.366(−3)	5.896(−3)	3.070(−2)	1.583(−1)	3.571(−2)	1.973(−1)
Fe^{14+}	5.636(−4)	7.860(−3)	5.063(−2)	1.753(−1)	1.209(−1)	1.934(−1)
Co^{15+}	9.588(−4)	6.088(−3)	6.343(−2)	2.017(−1)	3.882(−1)	1.544(−2)
Ni^{16+}	1.245(−3)	9.965(−3)	7.187(−2)	2.085(−1)	1.244(−1)	3.076(−1)
Cu^{17+}	2.213(−3)	2.605(−2)	8.267(−2)	2.375(−1)	5.413(−1)	1.318(−1)
Zn^{18+}	3.351(−3)	1.588(−2)	1.090(−2)	2.493(−1)	2.751(−1)	5.147(−1)
Kr^{24+}	2.586(−2)	5.166(−2)	3.166(−1)	3.618(−1)	5.225(−1)	1.313(+0)
Mo^{30+}	2.112(−2)	1.513(−1)	5.414(−1)	5.273(−1)	1.275(+0)	1.917(+0)
Xe^{42+}	9.924(−2)	2.073(−1)	1.331(+0)	1.017(+0)	2.607(+0)	4.419(+0)
	E_1	E_2	E_3	E_4	E_5	E_6
Al^{1+}	4.937(+3)	1.395(+4)	8.258(+4)	1.103(+5)	···	···
Si^{2+}	1.162(+2)	5.721(+3)	3.477(+4)	1.176(+5)	3.505(+6)	···
P^{3+}	1.532(+3)	2.588(+3)	7.095(+3)	4.171(+4)	1.477(+5)	1.083(+6)
S^{4+}	1.180(+3)	6.443(+3)	2.264(+4)	1.530(+5)	3.564(+5)	···
Cl^{5+}	1.010(+3)	3.305(+3)	1.717(+4)	8.541(+4)	2.098(+5)	2.381(+6)
Ar^{6+}	1.469(+3)	5.106(+3)	2.347(+4)	1.104(+5)	2.415(+5)	2.713(+6)
K^{7+}	1.915(+3)	6.277(+3)	3.614(+4)	1.467(+5)	2.860(+5)	3.142(+6)
Ca^{8+}	1.590(+3)	7.651(+3)	4.282(+4)	2.047(+5)	3.459(+5)	3.715(+6)
Sc^{9+}	3.767(+3)	1.589(+4)	5.182(+4)	2.698(+5)	5.686(+5)	4.220(+6)
Ti^{10+}	2.485(+3)	1.024(+4)	7.455(+4)	3.173(+5)	9.210(+5)	4.932(+6)
V^{11+}	3.489(+3)	1.748(+4)	8.329(+4)	3.717(+5)	7.715(+5)	5.480(+6)
Cr^{12+}	3.264(+3)	1.786(+4)	1.155(+5)	5.017(+5)	1.482(+6)	6.212(+6)
Mn^{13+}	3.889(+3)	1.914(+4)	1.155(+5)	4.511(+5)	3.366(+6)	7.114(+6)
Fe^{14+}	3.628(+3)	2.489(+4)	1.405(+5)	5.133(+5)	5.018(+6)	8.689(+6)
Co^{15+}	4.456(+3)	2.764(+4)	1.538(+5)	5.872(+5)	7.474(+6)	2.795(+7)
Ni^{16+}	4.018(+3)	3.701(+4)	1.603(+5)	6.190(+5)	5.227(+6)	1.031(+7)
Cu^{17+}	6.663(+3)	3.949(+4)	2.018(+5)	7.130(+5)	8.237(+6)	1.545(+7)
Zn^{18+}	7.215(+3)	3.479(+4)	2.271(+5)	7.631(+5)	6.263(+6)	1.210(+7)
Kr^{24+}	1.394(+4)	5.569(+4)	3.888(+5)	1.303(+6)	7.236(+6)	1.728(+7)
Mo^{30+}	1.491(+4)	1.200(+5)	5.373(+5)	1.993(+6)	1.052(+7)	2.507(+7)
Xe^{42+}	1.454(+4)	1.940(+5)	1.095(+6)	4.201(+6)	1.732(+7)	4.164(+7)

as we illustrate, the results of Dube & LaGattuta (1987), which are for 2p promotions only, lie well *above* those of Mazzotta et al. (1998) (and Arnaud & Raymond 1992) and so it appears that the contribution from 2p promotions has been omitted in practice. We also see that the results of Dube & LaGattuta (1987) are approximately a factor of two larger than our contribution from 2p promotions.

As we move to lower temperatures, the usual drop-off of the Mazzotta et al. (1998) data is observed in Fig. 2 because, for this case, the lowest temperature for which explicit results existed previously was at 4×10^5 K, due to Jacobs et al. (1977a). This is sufficient for electron-collisional plasmas, where the peak abundance of Fe^{14+} is at a few times 10^6 K, but not for photoionized plasmas where results are required down to 10^4 K. The low-temperature DR contribution shown here is up to an order of magnitude larger than the RR contribution at photoionized plasma temperatures (10^4–10^5 K), which translates into an order of magnitude increase in the total recombination rate coefficient which has been used to-date to model the ionization balance in photoionized plasmas. This is a characteristic of *all* Fe ions from Na-like (Altun et al. 2006) through to Ar-like (Badnell 2006c,d).

Our RR results for Fe^{14+}, also shown in Fig. 2, follow the well-tested approach of Badnell (2006b). Those recommended by Mazzotta et al. (1998) are just those of Shull & van Steenberg (1982) who, for Fe, simply retabulated the fit coefficients generated by Woods et al. (1981) which are stated to be accurate to better than 10% over $2.45 \times 10^5 < T < 3.92 \times 10^6$ K – no indication of the error outside of this range was given. But, like Aldrovandi & Péquignot (1973), and so Shull & van Steenburg (1982), Woods et al. (1981) fitted their RR rate coefficients to a single constant power of T, i.e. T^n, with n optimized for the temperature range of interest. As can be seen by the examination of Eq. (6), any results based on such a functional form must diverge increasingly from the true physical temperature dependence at

Table 2. RR fitting coefficients (see Eqs. (6, 7)) A (cm^3 s^{-1}), $T_{0,1,2}$ (K), B and C (the latter two are dimensionless) for ground state total RR rate coefficients of Mg-like ions.

Ion	A	B	T_0	T_1	C	T_2
Al^{1+}	1.035(−09)	0.6535	4.623(−2)	1.564(+09)	0.1261	1.533(+05)
Si^{2+}	1.964(−10)	0.6287	7.712(+00)	2.951(+07)	0.1523	4.804(+05)
P^{3+}	1.933(−10)	0.6235	3.527(+01)	2.694(+07)	0.1168	7.395(+05)
S^{4+}	2.615(−10)	0.6343	6.238(+01)	2.803(+07)	0.0773	1.059(+06)
Cl^{5+}	2.841(−10)	0.6367	1.244(+02)	3.039(+07)	0.0520	1.363(+06)
Ar^{6+}	3.370(−10)	0.6409	1.836(+02)	3.323(+07)	0.0320	1.717(+06)
K^{7+}	3.856(−10)	0.6423	2.598(+02)	3.572(+07)	0.0196	2.208(+06)
Ca^{8+}	4.641(−10)	0.6469	3.097(+02)	4.220(+07)	···	···
Sc^{9+}	4.471(−10)	0.6410	5.095(+02)	4.349(+07)	···	···
Ti^{10+}	4.441(−10)	0.6360	7.614(+02)	4.514(+07)	···	···
V^{11+}	4.627(−10)	0.6343	1.006(+03)	4.695(+07)	···	···
Cr^{12+}	5.026(−10)	0.6344	1.204(+03)	4.866(+07)	···	···
Mn^{13+}	5.037(−10)	0.6283	1.619(+03)	5.222(+07)	···	···
Fe^{14+}	5.398(−10)	0.6295	1.881(+03)	5.429(+07)	···	···
Co^{15+}	5.382(−10)	0.6247	2.441(+03)	5.812(+07)	···	···
Ni^{16+}	5.718(−10)	0.6246	2.783(+03)	6.091(+07)	···	···
Cu^{17+}	6.038(−10)	0.6244	3.166(+03)	6.420(+07)	···	···
Zn^{18+}	6.192(−10)	0.6223	3.743(+03)	6.775(+07)	···	···
Kr^{24+}	8.197(−10)	0.6230	6.620(+03)	9.048(+07)	···	···
Mo^{30+}	9.700(−10)	0.6196	1.128(+04)	1.189(+08)	···	···
Xe^{42+}	1.483(−09)	0.6294	1.863(+04)	1.819(+08)	···	···

both lower and higher temperatures outside of the limited temperature range of validity of the fit.

In Fig. 3 we compare our *LS*-coupling and MCBP total dielectronic recombination rate coefficients for Al^+ with the results obtained from the fitting data provided by Mazzotta et al. (1998). This is based on the Landini & Monsignori Fossi (1990) extrapolation of the results of fits of Shull & van Steenberg (1982) to the low-charge (Si, S) DR results of Jacobs et al. (1977b, 1979). The agreement between our intermediate-coupling MCBP results and those of Mazzotta et al. (1998) is very good for the high temperature peak. There is a low temperature peak which, of course, is not described by the Mazzotta et al. (1998) fit. This low temperature contribution has been considered by Nussbaumer & Storey (1986). The lowest autoionizing states are from the $3s3p^2$ configuration of neutral Al. The ^{2}S and ^{2}P terms are observed (see NIST) but the ^{2}D is not. Clearly, we cannot use the Al^+ target energies here. So, we adjusted the position of these neutral Al terms to the observed values, and shifting the ^{2}D consistently with these leaves it just bound. Since it is not possible to say theoretically whether the ^{2}D term is bound or not, Nussbaumer & Storey (1986) gave two sets of results – with and without this ^{2}D contribution. We see that our low temperature peak falls between their two sets of results. Our *LS*-coupling results are still in close agreement with our intermediate coupling results down to the low temperature peak, which is still larger than the contribution from RR down to 10^3 K. The RR data shown in Fig. 3 is from Landini & Monsignori Fossi (1990) and it is an extrapolation of the results of the retabulation by Shull & van Steenberg of the fits to the low-charge ion results of Aldrovandi & Péquignot (1973). Again, the original fits of Aldrovandi & Péquignot (1973) were temperature range restricted, but Landini & Monsignori Fossi (1990) give no such indication for their derived fits. This extrapolation probably accounts for the factor of two difference from our RR results.

In Fig. 4 we make comparisons for Si^{2+}. The high temperature DR peak (10^5 K) determined from the fit of Mazzotta et al. (1998), based on the results of Jacobs et al. (1977b), is in very close agreement with our MCBP (and *LS*-coupling) results. There is a very large DR contribution at low temperatures arising from the $3s3p3d\ ^2F_{7/2}$ level, which lies only about 80 cm^{-1} above the ionization limit (the $J = 5/2$ lies 160 cm^{-1} below) with a width of about 14 cm^{-1}. This level is "*LS*-allowed". There are a number of other higher levels nearby, but they are forbidden to autoionize in *LS*-coupling – they are discussed in detail by Nussbaumer & Storey (1986). Their DR calculations were basically *LS*-coupling ones and they treated this ^{2}F term as bound. (They did allow for spin-orbit mixing, semi empirically, via their "weak interaction" approximation.) If we treat the ^{2}F as bound then our low temperature results are consistent with those of Nussbaumer & Storey (1986). Our RR rate coefficients are in good agreement with those given by Aldrovandi & Péquignot (1973), especially at lower temperatures where RR would normally dominate.

In Fig. 5 we make comparisons for S^{4+}. At the high temperature DR peak (10^5 K) there is close agreement between our *LS*-coupling and MCBP intermediate coupling results with the results of Badnell (1991), who did not provide results below 3×10^4 K, and which were the basis of the fits provided by of Mazzotta et al. (1998). Our *LS*-coupling results still provide a fairly good description of the low temperature DR contribution, which dominates over RR at photoionized plasma temperatures (a few times 10^4 K). There is much better agreement now between our RR results and those explicitly calculated by Aldrovandi & Péquignot (1973) for this ion.

In Fig. 6 we make comparisons for Ca^{8+}. In this case, our *LS*- and intermediate-coupling MCBP DR results differ increasingly at lower temperatures. The high temperature results of Jacobs et al. (1980), which form the basis of the Mazzotta et al. (1998) fits, peak a little higher. The RR rate coefficients are in reasonable agreement, given that the Shull & van Steenberg (1982) ones are based on interpolation (between S of Aldrovandi & Péquignot 1973; and Fe of Woods et al. 1981).

In Fig. 7 we make comparisons for Ni^{16+}. Our *LS*- and intermediate coupling MCBP total dielectronic recombination

Table 3. Final state level-resolved DR+RR rate coefficients from the ground state of Fe^{14+} to the lowest 24 levels of Fe^{13+}. Here, C_1: $3s^23p$, C_2: $3s3p^2$, C_3: $3s^23d$, C_4: $3p^3$ and C_5: 3s3p3d.

T(K)	$C_1\,^2P_{1/2}$	$C_1\,^2P_{3/2}$	$C_2\,^4P_{1/2}$	$C_2\,^4P_{3/2}$	$C_2\,^4P_{5/2}$	$C_2\,^2D_{3/2}$	$C_2\,^2D_{5/2}$	$C_2\,^2S_{1/2}$
1.96(+3)	9.53(−12)	1.24(−11)	2.31(−12)	1.06(−12)	2.74(−12)	2.74(−11)	2.46(−11)	1.45(−11)
3.92(+3)	1.09(−11)	9.27(−12)	3.44(−12)	2.27(−12)	3.80(−12)	3.01(−11)	2.66(−11)	1.87(−11)
9.80(+3)	9.33(−12)	7.61(−12)	4.28(−12)	4.61(−12)	3.98(−12)	1.97(−11)	1.76(−11)	1.14(−11)
1.96(+4)	6.19(−12)	6.89(−12)	4.06(−12)	4.76(−12)	4.14(−12)	1.21(−11)	1.24(−11)	6.29(−12)
3.92(+4)	3.88(−12)	5.69(−12)	3.08(−12)	3.83(−12)	3.77(−12)	7.02(−12)	8.57(−12)	3.42(−13)
9.80(+4)	2.21(−12)	3.94(−12)	1.89(−12)	2.48(−12)	2.77(−12)	3.53(−12)	5.11(−12)	1.71(−12)
1.96(+5)	1.41(−12)	2.67(−12)	1.12(−12)	1.50(−12)	1.74(−12)	2.00(−12)	3.05(−12)	9.86(−13)
3.92(+5)	8.37(−13)	1.63(−12)	5.54(−13)	7.49(−13)	8.82(−13)	9.90(−13)	1.55(−12)	4.95(−13)
9.80(+5)	4.05(−13)	8.02(−13)	1.76(−13)	2.39(−13)	2.85(−13)	3.33(−13)	5.24(−13)	1.62(−13)
1.96(+6)	2.41(−13)	4.77(−13)	6.76(−14)	9.19(−14)	1.09(−13)	1.37(−13)	2.16(−13)	6.40(−14)
3.92(+6)	1.45(−13)	2.89(−13)	2.49(−14)	3.39(−14)	4.06(−14)	5.52(−14)	8.65(−14)	2.45(−14)
9.80(+6)	7.30(−14)	1.45(−13)	6.49(−15)	8.80(−15)	1.06(−14)	1.63(−14)	2.53(−14)	7.01(−15)
1.96(+7)	4.05(−14)	8.07(−14)	2.32(−15)	3.14(−15)	3.78(−15)	6.33(−15)	9.79(−15)	2.89(−15)
3.92(+7)	2.09(−14)	4.15(−14)	8.28(−16)	1.11(−15)	1.35(−15)	2.40(−15)	3.71(−15)	1.21(−15)
9.80(+7)	7.66(−15)	1.53(−14)	2.13(−16)	2.82(−16)	3.41(−16)	6.48(−16)	9.96(−16)	4.72(−16)
1.96(+8)	3.30(−15)	6.58(−15)	7.64(−17)	1.00(−16)	1.21(−16)	2.36(−16)	3.62(−16)	2.29(−16)
3.92(+8)	1.34(−15)	2.67(−15)	2.75(−17)	3.53(−17)	4.28(−17)	8.48(−17)	1.30(−16)	1.08(−16)
T(K)	$C_2\,^2P_{1/2}$	$C_2\,^2P_{3/2}$	$C_3\,^2D_{3/2}$	$C_3\,^2D_{5/2}$	$C_4\,^2D_{3/2}$	$C_4\,^2D_{5/2}$	$C_4\,^4S_{3/2}$	$C_4\,^2P_{1/2}$
1.96(+3)	1.85(−11)	2.06(−11)	1.22(−11)	1.62(−11)	1.55(−12)	2.06(−12)	4.25(−14)	2.05(−12)
3.92(+3)	2.03(−11)	2.67(−11)	1.35(−11)	1.57(−11)	1.58(−12)	1.06(−12)	4.81(−14)	1.16(−12)
9.80(+3)	1.07(−11)	1.52(−11)	2.22(−11)	2.78(−11)	1.12(−12)	6.52(−13)	5.56(−14)	1.15(−12)
1.96(+4)	5.31(−12)	7.57(−12)	1.94(−11)	2.70(−11)	9.30(−13)	8.71(−13)	1.31(−13)	1.34(−12)
3.92(+4)	2.69(−12)	3.90(−12)	1.18(−11)	1.76(−11)	1.07(−12)	1.80(−12)	5.83(−13)	1.29(−12)
9.80(+4)	1.32(−12)	2.04(−12)	5.11(−12)	7.98(−12)	1.29(−12)	2.88(−12)	1.19(−12)	1.01(−12)
1.96(+5)	7.69(−13)	1.23(−12)	2.69(−12)	4.27(−12)	9.69(−13)	2.32(−12)	9.75(−13)	6.81(−13)
3.92(+5)	3.91(−13)	6.36(−13)	1.39(−12)	2.21(−12)	5.34(−13)	1.33(−12)	5.54(−13)	3.66(−13)
9.80(+5)	1.28(−13)	2.12(−13)	5.67(−13)	8.90(−13)	1.81(−13)	4.69(−13)	1.91(−13)	1.24(−13)
1.96(+6)	5.03(−14)	8.31(−14)	2.83(−13)	4.41(−13)	7.10(−14)	1.87(−13)	7.52(−14)	4.90(−14)
3.92(+6)	1.88(−14)	3.10(−14)	1.38(−13)	2.15(−13)	2.65(−14)	7.02(−14)	2.81(−14)	1.83(−14)
9.80(+6)	5.05(−15)	8.15(−15)	5.04(−14)	7.72(−14)	6.92(−15)	1.84(−14)	7.35(−15)	4.79(−15)
1.96(+7)	1.89(−15)	2.93(−15)	2.19(−14)	3.34(−14)	2.47(−15)	6.60(−15)	2.63(−15)	1.71(−15)
3.92(+7)	7.23(−16)	1.04(−15)	8.98(−15)	1.37(−14)	8.79(−16)	2.35(−15)	9.34(−16)	6.09(−16)
9.80(+7)	2.15(−16)	2.66(−16)	2.57(−15)	3.92(−15)	2.33(−16)	5.96(−16)	2.37(−16)	1.55(−16)
1.96(+8)	8.90(−17)	9.42(−17)	9.61(−16)	1.46(−15)	7.89(−17)	2.11(−16)	8.39(−17)	5.47(−17)
3.92(+8)	3.73(−17)	3.34(−17)	3.51(−16)	5.33(−16)	2.79(−17)	7.47(−17)	2.97(−17)	1.94(−17)
T(K)	$C_5\,^4F_{3/2}$	$C_4\,^2P_{3/2}$	$C_4\,^4F_{5/2}$	$C_5\,^4F_{7/2}$	$C_5\,^4F_{9/2}$	$C_4\,^4P_{5/2}$	$C_5\,^4D_{3/2}$	$C_5\,^4D_{1/2}$
1.96(+3)	6.74(−13)	3.65(−12)	3.61(−13)	3.86(−14)	2.76(−20)	7.01(−11)	5.99(−11)	7.03(−11)
3.92(+3)	8.77(−13)	3.45(−12)	6.41(−13)	2.10(−13)	1.15(−17)	3.84(−11)	3.76(−11)	3.17(−11)
9.80(+3)	1.74(−12)	2.59(−12)	1.68(−12)	1.74(−12)	9.78(−15)	1.56(−11)	1.57(−11)	1.06(−11)
1.96(+4)	2.20(−12)	2.40(−12)	2.34(−12)	3.44(−12)	1.21(−13)	9.11(−12)	7.87(−12)	5.27(−12)
3.92(+4)	1.99(−12)	2.28(−12)	2.44(−12)	3.94(−12)	2.84(−13)	6.04(−12)	4.46(−12)	2.97(−12)
9.80(+4)	1.32(−12)	1.99(−12)	1.75(−12)	2.92(−12)	2.52(−13)	3.43(−12)	2.30(−12)	1.44(−12)
1.96(+5)	7.97(−13)	1.37(−12)	1.10(−12)	1.86(−12)	1.63(−13)	1.95(−12)	1.30(−12)	7.80(−13)
3.92(+5)	4.00(−13)	7.34(−13)	5.85(−13)	9.92(−13)	9.01(−14)	9.54(−13)	6.33(−13)	3.72(−13)
9.80(+5)	1.29(−13)	2.46(−13)	2.02(−13)	3.45(−13)	3.28(−14)	3.05(−13)	2.02(−13)	1.17(−13)
1.96(+6)	5.00(−14)	9.60(−14)	8.07(−14)	1.38(−13)	1.34(−14)	1.18(−13)	7.79(−14)	4.47(−14)
3.92(+6)	1.85(−14)	3.57(−14)	3.05(−14)	5.23(−14)	5.12(−15)	4.35(−14)	2.88(−14)	1.65(−14)
9.80(+6)	4.81(−15)	9.33(−15)	8.02(−15)	1.38(−14)	1.36(−15)	1.13(−14)	7.50(−15)	4.27(−15)
1.96(+7)	1.72(−15)	3.33(−15)	2.88(−15)	4.94(−15)	4.88(−16)	4.03(−15)	2.67(−15)	1.52(−15)
3.92(+7)	6.10(−16)	1.18(−15)	1.02(−15)	1.76(−15)	1.74(−16)	1.43(−15)	9.51(−16)	5.42(−16)
9.80(+7)	1.55(−16)	3.01(−16)	2.60(−16)	4.47(−16)	4.42(−17)	3.63(−16)	2.42(−16)	1.38(−16)
1.96(+8)	5.48(−17)	1.06(−16)	9.21(−17)	1.58(−16)	1.57(−17)	1.29(−16)	8.55(−17)	4.88(−17)
3.92(+8)	1.94(−17)	3.76(−17)	3.26(−17)	5.60(−17)	5.54(−18)	4.55(−17)	3.02(−17)	1.73(−17)

rate coefficients now agree better at lower temperatures, than for Ca^{8+}, illustrating the unpredictability of the representation of the low-temperature contribution and the validity of the coupling scheme in use. The high temperature results of Jacobs et al. (1980), which form the basis of the Mazzotta et al. (1998) fits, are in quite good agreement at high temperatures with our results. But, as with Fe, the contribution from 2p promotions (not included by Jacobs et al.) causes them to start to differ by 10^7 K. The RR fits given by Shull & van Steenburg are based on the extrapolation of the results of Woods et al. (1981) for Fe, which were valid down to a few times 10^5 K.

4. Summary

We have carried-out systematic calculations of DR data for the magnesium-like isoelectronic sequence as part of an assembly

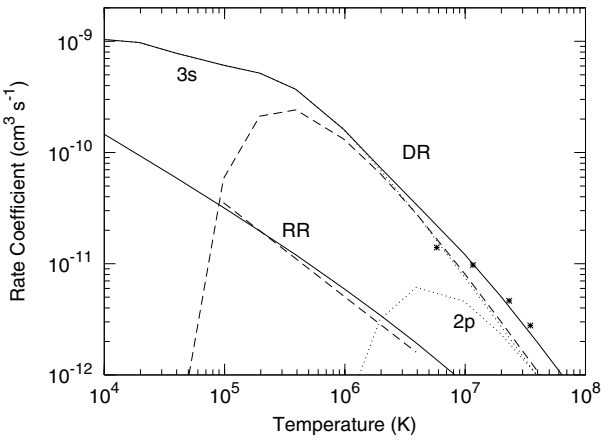

Fig. 2. Maxwellian-average rate coefficients for Fe^{14+}. Solid curves, total RR and DR (separate); dotted curves, DR for 3s and 2p promotions. All represent MCBP results from the current work. Long-dashed curves, DR taken from the fit of Mazzotta et al. (1998) and RR from Woods et al. (1981). Asterisks, DR for 2p promotions from Dube & LaGattuta (1987).

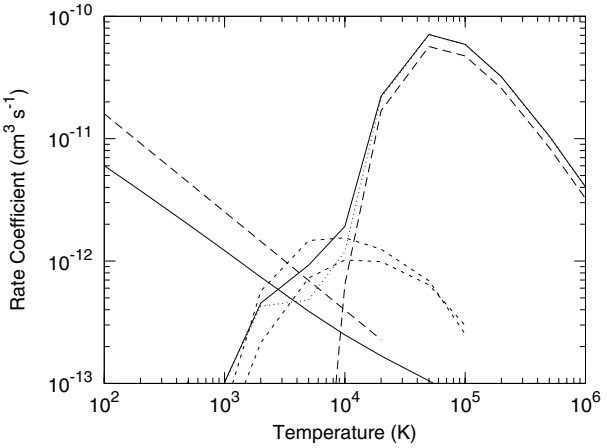

Fig. 3. Maxwellian-average rate coefficients for Al^+. Solid curves, total MCBP RR and DR (separate); dotted curve, *LS*-coupling DR. All represent MCBP results from the current work. Long-dashed curves, DR taken from the fit of Mazzotta et al. (1998) and RR from Landini & Monsignori Fossi (1990). Short-dashed curves, DR from Nussbaumer & Storey (1986).

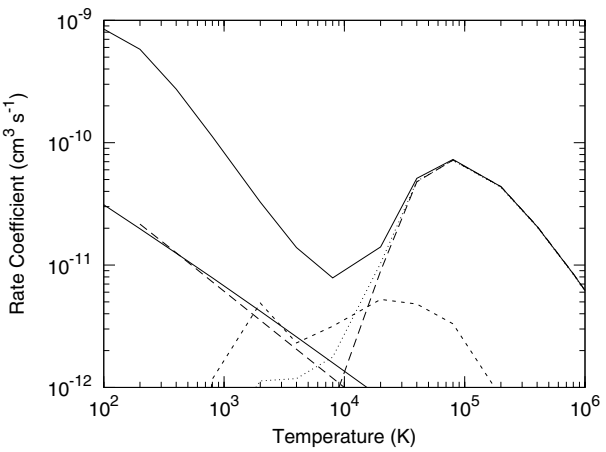

Fig. 4. Maxwellian-average rate coefficients for Si^{2+}. Solid curves, total MCBP RR and DR (separate); dotted curve, *LS*-coupling DR. All represent MCBP results from the current work. Long-dashed curves, DR taken from the fit of Mazzotta et al. (1998), based-on the work of Jacobs et al. (1977b), and RR from Aldrovandi & Péquignot (1973). Short-dashed curve, DR from Nussbaumer & Storey (1986).

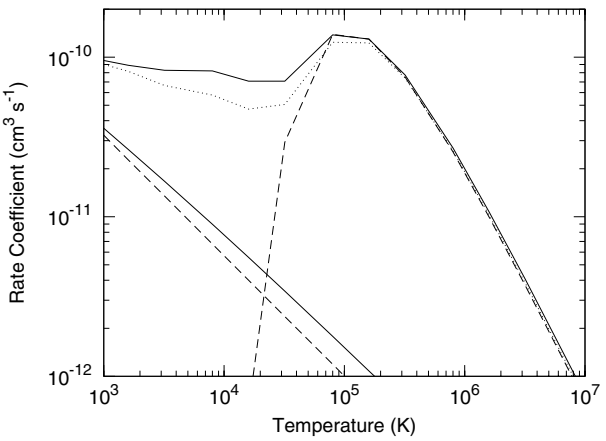

Fig. 5. Maxwellian-average rate coefficients for S^{4+}. Solid curves, total MCBP RR and DR (separate); dotted curve, *LS*-coupling DR. All represent MCBP results from the current work. Long-dashed curves, DR taken from the fit of Mazzotta et al. (1998), based-on the work of Badnell (1991), and RR from Aldrovandi & Péquignot (1973).

of a DR database necessary for the modelling of dynamic finite-density plasmas (Badnell et al. 2003). Calculations were carried-out in a multi-configuration intermediate coupling Breit-Pauli approximation for all ions for Al^+ to Zn^{18+}, as well as Kr^{24+}, Mo^{30+}, and Xe^{42+} using non-relativistic (up to Zn) and semi-relativistic (from Zn) radial functions. Complementary RR data have also been calculated and archived. We have presented selected total rate coefficients for some ions of interest in Figs. 3 to 7 and have made comparisons, where possible, with the recommended DR date provided by Mazzotta et al. (1998). Again, we have found large disagreements from this comparison for the electron temperatures below $\sim 5 \times 10^5 Z^2$ K, which is important for photoionized plasmas. The lack of other experimental and theoretical data in the literature prevents us from making further comparisons.

We have produced level-resolved final-state DR and RR rate coefficients in a form which will be useful for the modellers of both astrophysical and fusion plasmas, and these are available at `http://www-cfadc.phy.ornl.gov/data_and_codes`). Although our approximations are such that each final-state level-resolved DR rate coefficient may not be as highly accurate as some of the most sophisticated techniques available today, we have calculated a consistent set of data over a wide range of electron temperatures and for a large number of atomic ions in order to maximize the available information for modelling work. In order to facilitate the further application of our data, we have presented fits to our MCBP total DR and RR rate coefficients, separately.

Our high-temperature total rate coefficients should be accurate to better than ~20%. The main uncertainty is due to uncertainties in describing the underlying atomic structure, e.g. radiative rates. At low temperatures, typical of photoionized plasmas, the main uncertainty is due to the uncertainty in position of near threshold resonances. On-going and future work for further M-shell ions is to be focussed on total rate coefficients, especially for photoionized plasmas. The extension of the partial database is not yet warranted by modelling demands due to

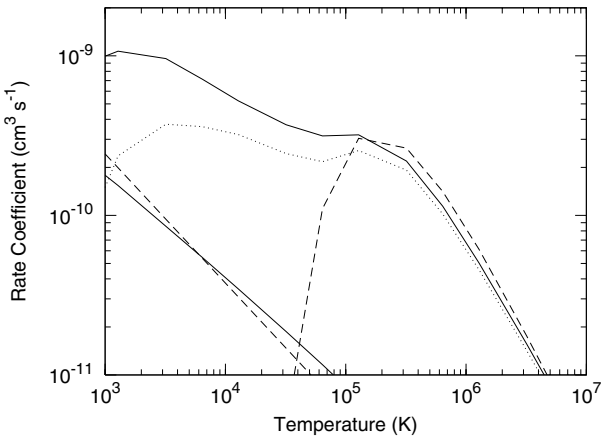

Fig. 6. Maxwellian-average rate coefficients for Ca^{8+}. Solid curves, total MCBP RR and DR (separate); dotted curve, *LS*-coupling DR. All represent MCBP results from the current work. Long-dashed curves, DR taken from the fit of Mazzotta et al. (1998), based-on the work of Jacobs et al. (1980), and RR from Shull & van Steenberg (1982).

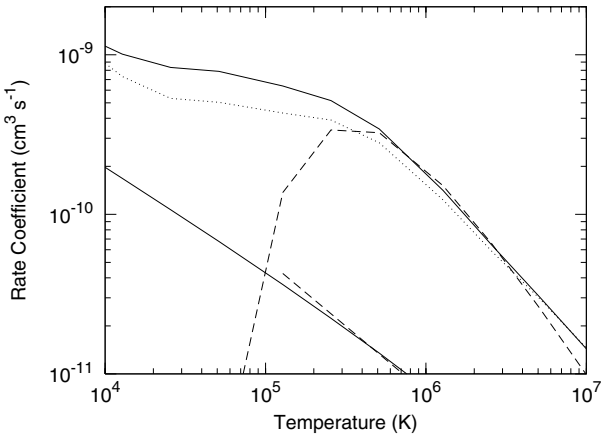

Fig. 7. Maxwellian-average rate coefficients for Ni^{16+}. Solid curves, total MCBP RR and DR (separate); dotted curve, *LS*-coupling DR. All represent MCBP results from the current work. Long-dashed curves, DR taken from the fit of Mazzotta et al. (1998), based-on the work of Jacobs et al. (1980), and RR from Shull & van Steenberg (1982).

the complexity of the atomic structure and, indeed, the demands upon atomic physics to describe it.

Acknowledgements. This work was supported in part by the US Department of Energy to Auburn University. Z.A. thanks the Turkish State Planning Organization (DPT) for a local computing grant.

References

Aldrovandi, S. M. V., & Péquignot, D. 1973, A&A, 25, 137
Altun, Z., Yumak, A., Badnell, N. R., Colgan, J., & Pindzola, M. S. 2004, A&A, 420, 775
Altun, Z., Yumak, A., Badnell, N. R., Loch, S. D., & Pindzola, M. S. 2006, A&A, 447, 1165
Arnaud, M., & Raymond, J. 1992, ApJ, 398, 394
Arnaud, M., & Rothenflug, R. 1985, A&AS, 60, 425
Badnell, N. R. 1986, J. Phys. B, 19, 3827
Badnell, N. R. 1991, ApJ, 379, 356
Badnell, N. R. 1997, J. Phys. B, 30, 1
Badnell, N. R. 2006a, A&A, 447, 389
Badnell, N. R. 2006b, ApJS, 167, 334
Badnell, N. R. 2006c, J. Phys. B, 39, 4825
Badnell, N. R. 2006d, ApJ, 651, L73
Badnell, N. R., O'Mullane, M., Summers, H. P., et al. 2003, A&A, 406, 1151
Bryans, P., Badnell, N. R., Gorczyca, T. W., et al. 2006, ApJS, 167, 343
Bautista, M. A., & Badnell, N. R. 2007, A&A, 466, 755
Burgess, A. 1964, ApJ, 139, 776
Burgess, A., & Summers, H. P. 1969, ApJ, 157, 1007
Chen, M. H. 1985, Phys. Rev. A, 31, 1449
Chen, M. H. 1987, Phys. Rev. A, 35, 4129
Chen, M. H. 2002, Phys. Rev. A, 66, 052715
Colgan, J., Pindzola, M. S., Whiteford, A. D., & Badnell, N. R. 2003, A&A, 412, 597
Colgan, J., Pindzola, M. S., & Badnell, N. R. 2004, A&A, 417, 1183
Dube, M. P., Rasoanaivo, R., & Hahn, Y. 1985, J. Quant. Spectrosc. Radiat. Transfer, 33, 13
Dube, M. P., & LaGattuta, K. J. 1987, J. Quant. Spectrosc. Radiat. Transfer, 38, 311
Ferland, G. J., Korista, K. T., Verner, D. A., et al. 1998, PASP, 110, 761
Gu, M. F. 2003a, ApJ, 590, 1131
Gu, M. F. 2003b, ApJ, 582, 1241
Gu, M. F. 2004, ApJS, 153, 389
Hahn, Y. 1989, J. Quant. Spectrosc. Radiat. Transfer, 41, 315
Jacobs, V. L., Davis, J., Kepple, P. C., & Blaha, M. 1977a, ApJ, 211, 605
Jacobs, V. L., Davis, J., Kepple, P. C., & Blaha, M. 1977b, ApJ, 215, 690
Jacobs, V. L., Davis, J., Rogerson, J. E., & Blaha, M. 1979, ApJ, 230, 627
Jacobs, V. L., Davis, J., Rogerson, J. E., et al. 1980, ApJ, 239, 1119
Kraemer, S. B., Ferland, G. J., & Gabel, J. R. 2004, ApJ, 604, 556
Landini, M., & Monsignori Fossi, B. C. 1990, A&AS, 82, 229
Landini, M., & Monsignori Fossi, B. C. 1991, A&AS, 91, 183
Lukić, D. V, Schnell, M., Savin, D. W, et al. 2007, ApJ, 664, 1244
Mattioli, M. 1988, Euratom-CEA Report No. EUR-CEA-FC-1346
Mazzotta, P., Mazzitelli, G., Colafrancesco, S., & Vittorio, N. 1998, A&AS, 133, 403
Mitnik, D. M., Pindzola, M. S., & Badnell, N. R. 1999, Phys. Rev. A, 59, 3592
Mitnik, D. M., & Badnell, N. R. 2004, A&A, 425, 1153
Müller, A. 1999, Int. J. Mass Spectrom, 192, 9
Netzer, H. 2004, ApJ, 604, 551
Netzer, H., Kaspi, S., Behar, E., et al. 2003, ApJ, 599, 933
NIST web page `http://physics.nist.gov/PhysRefData/ASD/`
Nussbaumer, H., & Storey, P. J. 1983, A&A, 126, 75
Nussbaumer, H., & Storey, P. J. 1984, A&AS, 56, 293
Nussbaumer, H., & Storey, P. J. 1986, A&AS, 64, 545
Nussbaumer, H., & Storey, P. J. 1987, A&AS, 69, 123
Pindzola, M. S., Badnell, N. R., & Griffin, D. C. 1992, Phys. Rev. A, 46, 5725
Savin, D. W., & Laming, J. M. 2002, ApJ, 566, 1166
Schmidt, E. W. 2007, private communication
Schmidt, E. W., Schippers, S., Müller, A., et al. 2006, ApJ, 641, L157
Shull, J. M., & van Steenberg, M. 1982, ApJS, 48, 95
Summers, H. P. 2003, ADAS User Manual (v2.6), available from `http://adas.phys.strath.ac.uk/adas/docs/manual`
Woods, D. T., Shull, J. M., & Sarazin, C. L. 1981, ApJ, 249, 399
Zatsarinny, O., Gorczyca, T. W., Korista, K. T., Badnell, N. R., & Savin, D. W. 2003, A&A, 412, 587
Zatsarinny, O., Gorczyca, T. W., Korista, K. T., Badnell, N. R., & Savin, D. W. 2004a, A&A, 417, 1173
Zatsarinny, O., Gorczyca, T. W., Korista, K. T., Badnell, N. R., & Savin, D. W. 2004b, A&A, 426, 699
Zatsarinny, O., Gorczyca, T. W., Fu, J., et al. 2006, A&A, 447, 379